

Dissipative qutrit-mediated stable charging

Chen-yi Zhang¹ and Jun Jing^{1,*}

¹*School of Physics, Zhejiang University, Hangzhou 310027, Zhejiang, China*

(Dated: May 2, 2025)

In this work, we propose a stable charging scheme mediated by a dissipative three-level system, which allows a unidirectional energy flow from the external power source to a finite-dimensional quantum battery. By virtue of the dissipation, the battery avoids the spontaneous discharging induced by the time-reversal symmetry in any unitary charging scheme. Irrespective to the initial state, the battery can be eventually stabilized at the maximal-ergotropy state as long as the charger-battery interaction is present. We use a Dyson series of Lindbladian superoperator to obtain an effective master equation to describe the battery dynamics and extract the optimization condition for charging efficiency. Also it proves that the Fermi's golden rule can adapt to the non-Hermitian Hamiltonian. We justify the outstanding performance of our charging scheme when applied to the finite-size system with a uniform energy ladder operator, the large spin battery, and the truncated harmonic oscillator battery.

I. INTRODUCTION

As a microscopic unit for energy storage, quantum battery [1] has recently received remarkable attention as both a promising energy supply device for quantum technology [2] and a tool to develop the wide application of quantum thermodynamics [3–6]. Since formally introduced by Alicki and Fannes [7], a lot of efforts have been devoted to studying the role of quantum resources such as quantum correlation and quantum coherence in the charging performance of various quantum batteries [7–14]. It is found that the collective charging schemes could achieve a super-extensive scaling in power, which supports that the quantum correlation provides a dramatic boost to the charging efficiency of the parallel charging schemes [15–17]. Quantum speed up in charging can also be found in a single high-dimensional quantum battery via repeated collisions between chargers and battery [11, 18, 19]. In addition, quantum measurements on chargers can give rise to a more efficient charging performance than the measurement-free schemes and do not invoke the initial quantum coherence in both battery and chargers [20].

Numerous prototypes of quantum batteries have been developed in diverse models. The one-dimensional spin chain battery has been proposed in Ref. [16]. Then many investigations further extended the spin chain to the spin-ensemble systems [21–28]. For example, by mediating between the charger and battery both consisting of a spin ensemble through a magnon system, we can realize a long-range charging [21]. Dick model battery is another type of extensively studied model [10, 15, 29–31], which is based on the interaction between an ensemble of noninteracting two-level systems (TLSs) and a common cavity mode. The connection and distinction between the spin-charger and cavity-charger schemes were discussed in Ref. [22]. In addition to the spin systems, the bosonic

quantum battery based on an ensemble of harmonic oscillators (HOs) was proposed in Ref. [32] focusing on the charging precision, i.e., the variance of high-level population distribution.

Besides the charging efficiency, stabilizing a quantum battery at the charged (high-ergotropy) state is also crucial for the reliable operation over quantum batteries. Many conventional schemes have to immediately decouple the charger from the battery of a finite size when the latter reaches the fully charged state. If they remain coupled with each other, energy can flow back from the battery to the charger, degrading the charging-efficiency and the energy retention [10, 15, 29, 33, 34]. Extra operations have been designed to address this challenge. The Zeno-protection scheme applies sequential projective measurements on the high energy state of a two-level quantum battery [35]. The time-dependent Hamiltonian schemes use the stimulated Raman adiabatic passage to maintain a stable charged state [36, 37]. Nonlocal and strong chaotic correlation was demonstrated in a Sachdev-Ye-Kitaev quantum battery [38] to improve the charging stability, to name a few.

An alternative approach for stable charging is assisted by a dissipative charger connecting the battery and the external power source [39]. In that model that both charger and battery are identical HOs or TLSs, the energy and ergotropy of the battery can be stabilized at a finite value determined by the charger-battery coupling strength and the intensity of the external power source. However, the battery could not be stabilized at its highest energy level in such a setting. Introducing a common dissipative environment for the composite system of battery and charger and carefully designing their inner coupling strength and the dissipative rates can increase the steady energy in the battery [40].

In this work, we introduce an efficient and stable charging model that the charger is modeled as a dissipative Δ -type qutrit mediating between the external power source and the battery. The charger is coupled to the battery through the energy exchange interaction. By deriving an effective master equation for the battery using a pertur-

* Email address: jingjun@zju.edu.cn

bation technique for Lindbliadian superoperator, we find that a unidirectional energy flow from the external source to the battery is constructed due to the time-reversal symmetry breaking by the dissipative charger. We first consider the battery with a uniform energy ladder operator that is popular in many works[11, 41, 42]. Our scheme is characterized with universality in enhancing and holding the battery energy for any initial state [43] and does not require the charger to be decoupled from the battery after the charging is completed. We apply our scheme to more realistic scenarios by modeling quantum battery as a large spin and a truncated quantum harmonic oscillator. It is interesting to find that choosing an appropriate charger-battery coupling strength or adjusting it during the charging process can significantly boost the charging efficiency.

The rest of the paper is organized as follows. In Sec. II, we introduce our dissipative-mediated charging model. In Sec. III, we derive an effective master equation for the battery in a weak-driving regime (see appendix A for details) and obtain the optimization condition for charging efficiency. In a broader perspective, we actually develop an efficient technique to extend the Fermi's Golden rule to adapt to the non-Hermitian Hamiltonian. In Sec. IV, we discuss the large spin quantum battery. It is found that charging efficiency can be significantly boosted by optimizing the effective transition rate for special subspaces. In Sec. V, we discuss the truncated harmonic oscillator quantum battery. It is shown that by adjusting the charger-battery coupling strength according to the instantaneous state of the battery, the charging efficiency can be greatly enhanced. The conclusion is provided in Sec. VI.

II. MODEL

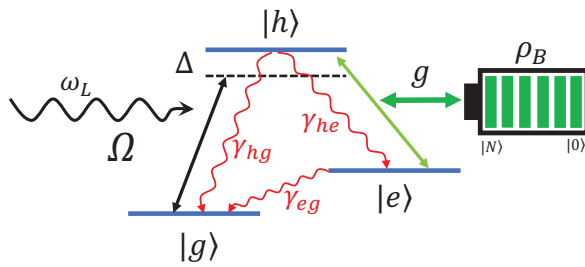


FIG. 1. Sketch of the source-charger-battery system. In our charging scheme, the dissipative Δ -type qutrit serves as the charger, that is driven by an external power source and transfers energy to the battery.

Our indirect charging model consists of a quantum battery of a finite size and a dissipative charger that is driven by an external power source. As shown in Fig. 1, the charger is a dissipative Δ -type qutrit. An external field directly drives the transition between levels $|g\rangle$ and $|h\rangle$. The quantum battery in Secs. II and III has $N + 1$

uniform energy levels with a bare Hamiltonian ($\hbar = 1$) $H_B = E \sum_{n=0}^N n|n\rangle\langle n|$. The charging process is switched on when the quantum battery couples to the qutrit via the transition $|e\rangle \leftrightarrow |h\rangle$. The full system Hamiltonian reads,

$$H = \omega_{hg}|h\rangle\langle h| + \omega_{eg}|e\rangle\langle e| + H_B + (\Omega|h\rangle\langle g|e^{-i\omega_L t} + gA^\dagger|e\rangle\langle h| + \text{H.c.}), \quad (1)$$

where ω_{ij} with $i, j = g, e, h$ is the level splitting between qutrit states $|i\rangle$ and $|j\rangle$. Ω and ω_L are the intensity and the frequency of the external field, respectively. g is the coupling strength between the charger and the battery. $A^\dagger = \sum_{n=0}^{N-1} A_n|n+1\rangle\langle n|$ is the creation operator of the battery, which satisfies $A^\dagger|N\rangle = A|0\rangle = 0$ and A_n is a dimensionless transition coefficient between $|n\rangle$ and $|n+1\rangle$. $A_{n \geq N} = 0$. In the rotating frame with respect to

$$U = \exp \{i [H_B + \omega_L|h\rangle\langle h| + (\omega_L - E)|e\rangle\langle e|] t\}, \quad (2)$$

the full Hamiltonian reads

$$H' = U H U^\dagger - i U \frac{\partial}{\partial t} U^\dagger = \Delta|h\rangle\langle h| + \delta|e\rangle\langle e| + \Omega(|h\rangle\langle g| + |g\rangle\langle h|) + g(A^\dagger|e\rangle\langle h| + A|h\rangle\langle e|) \quad (3)$$

with detunings $\Delta = \omega_{hg} - \omega_L$ and $\delta = \omega_{eg} + E - \omega_L$. When the charger is subject to a local dissipative environment, the evolution of the charger-battery system is governed by the master equation [44]:

$$\dot{\rho}(t) = -i[H', \rho(t)] + \sum_{ij=hg,he,eg} \mathcal{L}[L_{ij}]\rho(t), \quad (4)$$

where $L_{ij} = \sqrt{\gamma_{ij}}|j\rangle\langle i|$ is the Lindblad operator (quantum jump operator) from the qutrit level $|i\rangle$ to $|j\rangle$ with a decay rate γ_{ij} . $\mathcal{L}[o]$ is the Lindblad superoperator defined as $\mathcal{L}[o]\rho(t) \equiv o\rho(t)o^\dagger - 1/2\{o^\dagger o, \rho(t)\}$.

III. EFFECTIVE MASTER EQUATION

In our charging scheme, the mediator qutrit is initially prepared in its ground state $|g\rangle$. In the weak-driving regime $\Omega \ll \Delta, \gamma_{hg}$, one can suppose that the qutrit subject to a dissipative environment remains mostly in its ground state $\rho(t) \approx P_g \rho(t) P_g$, where $P_g \equiv |g\rangle\langle g|$. According to the master equation (4), the main mechanism underlying the indirect charging can be illustrated in the subspaces spanned by $\{|gn\rangle, |hn\rangle, |e(n+1)\rangle, |g(n+1)\rangle\}$ for $n < N$. As shown in Fig. 2(a), the system is driven from $|gn\rangle$ to $|hn\rangle$ through the external power source Ω and from $|hn\rangle$ to $|e(n+1)\rangle$ via the charger-battery interaction with a coupling strength gA_n . Subsequently, the spontaneous decay γ_{eg} induces a transition from $|e(n+1)\rangle$ to $|g(n+1)\rangle$. These processes constitute an effective unidirectional transition from $|gn\rangle$ to $|g(n+1)\rangle$, which can

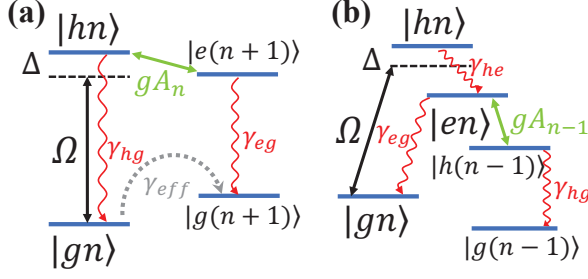


FIG. 2. (a) Main mechanism of our charging scheme. The external power source Ω , the charger-battery interaction gA_n , and the spontaneous decay γ_{eg} induces the transitions $|gn\rangle \rightarrow |hn\rangle$, $|hn\rangle \rightarrow |e(n+1)\rangle$, and $|e(n+1)\rangle \rightarrow |g(n+1)\rangle$, respectively. They give rise to an effective transition $|gn\rangle \rightarrow |g(n+1)\rangle$ with a rate γ_{eff} . (b) Leading-order transitions induced by the atomic spontaneous emissions from $|h\rangle$ to $|e\rangle$ and from $|e\rangle$ to $|g\rangle$. The decay channel indicated by γ_{he} is the main negative factor for charging.

be quantitatively described by the effective Lindblad operator in Eq. (A22):

$$L_{eg,n}^{\text{eff}} = \frac{\sqrt{\gamma_{eg}}\Omega gA_n}{g^2 A_n^2 - \tilde{\Delta}\tilde{\delta}} |g(n+1)\rangle\langle gn| \quad (5)$$

with $\tilde{\Delta} \equiv \Delta - i\gamma_{hg}/2 - i\gamma_{he}/2$ and $\tilde{\delta} \equiv \delta - i\gamma_{eg}/2$ the complex detunings. Due to the large-detuning condition, the decay from $|hn\rangle$ to $|gn\rangle$ contributes to a pure dephasing of the state $|gn\rangle$ in the leading order. The relevant effective Lindblad operator given by Eq. (A21) reads

$$L_{hg,n}^{\text{eff}} = \frac{\sqrt{\gamma_{hg}}\Omega\tilde{\delta}}{\tilde{\Delta}\tilde{\delta} - g^2 A_n^2} |gn\rangle\langle gn|. \quad (6)$$

In addition, the energy shift of $|gn\rangle$ induced by the weak driving and the charger-battery interaction can be described by the effective Hamiltonian

$$H_n^{\text{eff}} = -\Omega^2 \text{Re} \left(\frac{\tilde{\delta}}{\tilde{\Delta}\tilde{\delta} - g^2 A_n^2} \right) |gn\rangle\langle gn|. \quad (7)$$

The relevant details can be found in Appendix A.

By tracing out the qutrit from Eq. (4), the effective equation of motion of the battery is given by

$$\dot{\rho}_B(t) = -i[H_{\text{eff}}^B, \rho_B(t)] + \mathcal{L}[L_{hg,\text{eff}}^B]\rho_B(t) + \mathcal{L}[L_{eg,\text{eff}}^B]\rho_B(t), \quad (8)$$

where

$$\begin{aligned} H_{\text{eff}}^B &= \sum_{n=0}^N -\Omega^2 \text{Re} \left(\frac{\tilde{\delta}}{\tilde{\Delta}\tilde{\delta} - g^2 A_n^2} \right) |n\rangle\langle n| \\ &= -\Omega^2 \text{Re} \left(\frac{\tilde{\delta}}{\tilde{\Delta}\tilde{\delta} - AA^\dagger g^2} \right), \end{aligned} \quad (9)$$

and

$$L_{hg,\text{eff}}^B = \sum_{n=0}^N \frac{\sqrt{\gamma_{hg}}\Omega\tilde{\delta}}{\tilde{\Delta}\tilde{\delta} - g^2 A_n^2} |n\rangle\langle n| = \frac{\sqrt{\gamma_{hg}}\Omega\tilde{\delta}}{\tilde{\Delta}\tilde{\delta} - AA^\dagger g^2}, \quad (10a)$$

$$L_{eg,\text{eff}}^B = \sum_{n=0}^N \frac{\sqrt{\gamma_{eg}}\Omega gA_n}{g^2 A_n^2 - \tilde{\Delta}\tilde{\delta}} |n+1\rangle\langle n| = \frac{\sqrt{\gamma_{eg}}\Omega}{A^\dagger Ag^2 - \tilde{\Delta}\tilde{\delta}} A^\dagger. \quad (10b)$$

are the effective Hamiltonian and Lindblad operators in the battery Hilbert space, respectively. When expanding the coefficients of the effective Lindblad operators in terms of series

$$\begin{aligned} \langle gn|L_{hg,n}^{\text{eff}}|gn\rangle &= \sqrt{\gamma_{hg}} \sum_{k=0}^{\infty} \left(\frac{g^2 A_n^2}{\tilde{\Delta}\tilde{\delta}} \right)^k \frac{\Omega}{\tilde{\Delta}} \\ &= -\sqrt{\gamma_{hg}} \sum_{k=0}^{\infty} \Omega_{\text{eff}}^{(2k)}, \\ \langle g(n+1)|L_{eg,n}^{\text{eff}}|gn\rangle &= -\sqrt{\gamma_{eg}} \sum_{k=0}^{\infty} \left(\frac{g^2 A_n^2}{\tilde{\Delta}\tilde{\delta}} \right)^k \frac{gA_n}{\tilde{\delta}} \frac{\Omega}{\tilde{\Delta}} \\ &= -\sqrt{\gamma_{eg}} \sum_{k=0}^{\infty} \Omega_{\text{eff}}^{(2k+1)}, \end{aligned} \quad (11)$$

it is interesting to find that $\Omega_{\text{eff}}^{(l)}$'s are precisely the effective coupling strengths connecting $|i\rangle = |gn\rangle$ and $|f\rangle = |hn\rangle$ or $|e(n+1)\rangle$ up to the first order in Ω and l order in gA_n with respect to the non-Hermitian Hamiltonian in Eq. (A5):

$$\begin{aligned} \tilde{H}_n &= \tilde{H}_{0,n} + \tilde{V}_n, \\ \tilde{H}_{0,n} &= \tilde{\Delta}|hn\rangle\langle hn| + \tilde{\delta}|e(n+1)\rangle\langle e(n+1)|, \\ \tilde{V}_n &= gA_n(|hn\rangle\langle e(n+1)| + |e(n+1)\rangle\langle hn|). \end{aligned} \quad (12)$$

Particularly, they can be obtained by the constrained high-order Fermi's golden rules [45] with the form

$$\begin{aligned} \Omega_{\text{eff}}^{(l)} &= \sum_{m_1, m_2, \dots, m_l} \frac{\tilde{V}_{n,fm_{l-1}} \cdots \tilde{V}_{n,m_2m_1} \tilde{V}_{n,m_1i}}{(\tilde{E}_i - \tilde{E}_{m_1})(\tilde{E}_i - \tilde{E}_{m_2}) \cdots (\tilde{E}_i - \tilde{E}_{m_{l-1}})}, \end{aligned} \quad (13)$$

where $\tilde{V}_{n,m_i m_j} = \langle m_i|\tilde{V}_n|m_j\rangle$ with $m_i = hn, e(n+1)$ the intermediate states. $\tilde{E}_{m_i} = \langle m_i|\tilde{H}_{0,n}|m_i\rangle$ and $\tilde{E}_i = \langle gn|\tilde{H}_{0,n}|gn\rangle = 0$ are the diagonal elements of $\tilde{H}_{0,n}$. For an even l , $\Omega_{\text{eff}}^{(l)}$ represents the effective coupling strength for connecting $|gn\rangle$ and $|hn\rangle$ through the process $|gn\rangle \rightarrow |hn\rangle \rightarrow |e(n+1)\rangle \cdots \rightarrow |hn\rangle$. For an odd l , it represents the effective coupling strength for connecting $|gn\rangle$ and $|e(n+1)\rangle$ through the process $|gn\rangle \rightarrow |hn\rangle \rightarrow |e(n+1)\rangle \cdots \rightarrow |e(n+1)\rangle$. Similarly, the coefficient of the effective Hamiltonian (9) is the real part of the summation of all round trips about $|gn\rangle$.

The effective transition rate about $|gn\rangle \rightarrow |g(n+1)\rangle$

in Fig. 2(a) is given by

$$\begin{aligned} \gamma_{n,\text{eff}} &= |\langle g(n+1) | L_{eg,n}^{\text{eff}} | gn \rangle|^2 = \left| \frac{\sqrt{\gamma_{eg}} \Omega g A_n}{g^2 A_n^2 - \tilde{\Delta} \tilde{\delta}} \right|^2 \\ &= \frac{\gamma_{eg} \Omega^2}{g^2 A_n^2 + |\tilde{\Delta} \tilde{\delta}|^2 / (g^2 A_n^2) - 2 |\tilde{\Delta} \tilde{\delta}| \cos \phi}, \end{aligned} \quad (14)$$

where $\phi = \arg(\tilde{\Delta} \tilde{\delta})$. With fixed detunings $\tilde{\Delta}$ and $\tilde{\delta}$, one can find that the effective transition rate in the n th subspace can be optimized by setting

$$g_{\text{opt}}^2 A_n^2 = |\tilde{\Delta} \tilde{\delta}|. \quad (15)$$

The decay channel $|h\rangle \rightarrow |e\rangle$ plays a negative role in the charging efficiency through a higher-order process than $|e\rangle \rightarrow |g\rangle$ and $|h\rangle \rightarrow |g\rangle$ (see Appendix A). As the leading-order contribution depicted in Fig. 2(b), the system in the subspace is driven by the external power from $|gn\rangle$ to $|hn\rangle$ then decay from $|hn\rangle$ to $|en\rangle$ and then decay from $|en\rangle$ to $|gn\rangle$ will give rise to an effective dephasing on the state $|gn\rangle$ with a rate given by Eq. (A32). In a biased fluxonium system at about $0.05 \leq \Phi_{\text{ex}}/\Phi_0 \leq 0.15$, where Φ_{ex} and Φ_0 are the applied flux and flux quantum, respectively, γ_{he} is the same order in magnitude as γ_{eg} and is one order of magnitude smaller than γ_{hg} [46, 47], i.e. $\gamma_{eg} \approx \gamma_{he} \ll \gamma_{hg}$. With such a parametric setting, one can confirm that the dephasing rate caused by the process in Fig. 2(b) is negligible in comparison to that described by Eq. (6) for $|gn\rangle \rightarrow |hn\rangle \rightarrow |gn\rangle$ in Fig. 2(a). Similarly, the process that from $|gn\rangle$ to $|hn\rangle$ through the external driving, from $|hn\rangle$ to $|en\rangle$ through the spontaneous decay γ_{he} , from $|en\rangle$ to $|h(n-1)\rangle$ through the charger-battery interaction, and finally from $|h(n-1)\rangle$ to $|g(n-1)\rangle$ through the spontaneous decay γ_{hg} gives rise to an effective transition from $|gn\rangle$ to $|g(n-1)\rangle$ with a rate given by Eq. (A35). It is also negligible comparing to the effective transition rate in Eq. (14) under the condition $|\tilde{\Delta}| \gg |\tilde{\delta}|$ and $\gamma_{eg} \approx \gamma_{he}$. Consequently, the presence of a decay channel $|h\rangle \rightarrow |e\rangle$ does not significantly alter our unidirectional energy flow.

The justification of our charging scheme begins with a simple case with $A_n = 1$, resulting in uniform effective transition rates across all the subspaces. Substituting the optimized condition (15) to Eq. (14), it is found that the optimized effective transition rate reads

$$\gamma_{\text{eff}}^{\text{opt}} = \frac{\gamma_{eg} \Omega^2}{4 |\tilde{\Delta} \tilde{\delta}| \sin^2(\phi/2)}. \quad (16)$$

The performance of the charging protocol can be evaluated by the energy stored in the battery

$$\Delta E(t) \equiv \text{Tr}[H_B \rho_B(t)] - \text{Tr}[H_B \rho_B(0)], \quad (17)$$

and the ergotropy [48], the maximum amount of work that can be extracted from the battery via unitary transformation, which is defined as

$$\mathcal{E}(t) \equiv \text{Tr}[H_B(\rho_B(t))] - \text{Tr}[H_B \sigma(t)], \quad (18)$$

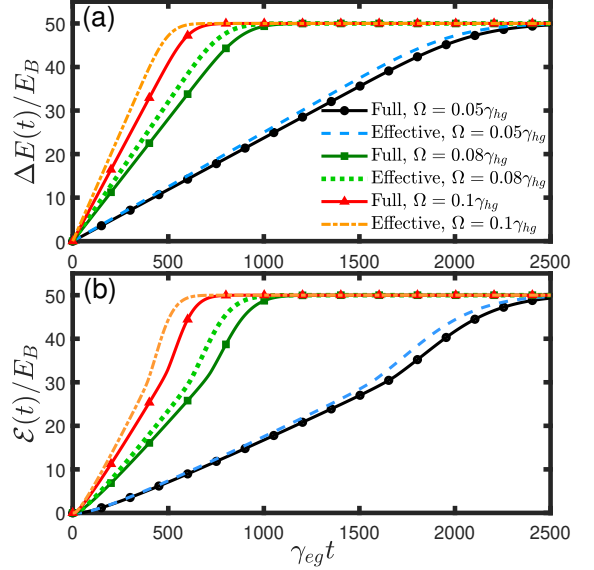


FIG. 3. Comparison between the dynamics obtained by the full master equation (4) and the effective master equation (8) of (a) battery energy $\Delta E(t)$ and (b) ergotropy $\mathcal{E}(t)$ as functions of $\gamma_{eg} t$ with various Ω . The coupling strength g satisfies the optimized condition (15). The battery size is set as $N = 50$. $\gamma_{he} = 0$, $\gamma_{hg} = 10\gamma_{eg} = 0.1E_B$, and $\Delta = 10\delta = 0.1E_B$.

Here $\sigma(t)$ is the passive state that is diagonal in the battery eigenstates basis with non-increasing eigenvalues of $\rho_B(t)$:

$$\sigma(t) = \sum_{n=0}^N \lambda_n(t) |n\rangle \langle n|, \quad \lambda_{n+1}(t) \leq \lambda_n(t) \quad (19)$$

Both energy and ergotropy saturate when the battery state approaches the maximal-ergotropy state $\rho_B \rightarrow |N\rangle \langle N|$. By virtue of the last term in Eq. (8) interpreted by Eq. (10b), our charging scheme can hold on that state without decoupling the charger from the battery after the charging process is completed.

In Fig. 3, we compare the dynamics of the battery energy $\Delta E(t)$ and ergotropy $\mathcal{E}(t)$ under the full master equation (4) and the effective master equation (8). The battery is initially prepared at its ground state $\rho_B(0) = |0\rangle \langle 0|$ with vanishing energy and ergotropy. It is found that for either energy in Fig. 3(a) or ergotropy in Fig. 3(b), the charging efficiency becomes higher under a stronger driving intensity Ω . On the other hand, the deviation between the effective dynamics and the full dynamics increases when Ω becomes larger and larger. It is due to the breakdown of the weak driving assumption.

A practical charging scheme can transform a high-energy yet zero-ergotropy state, e.g., the thermal state, to be a high-energy and high-ergotropy state. In Fig. 4(a) and 4(b), we demonstrate the charging performance for the initial thermal states with various inverse temperatures β by the stored energy $\Delta E(t)$ and ergotropy $\mathcal{E}(t)$,

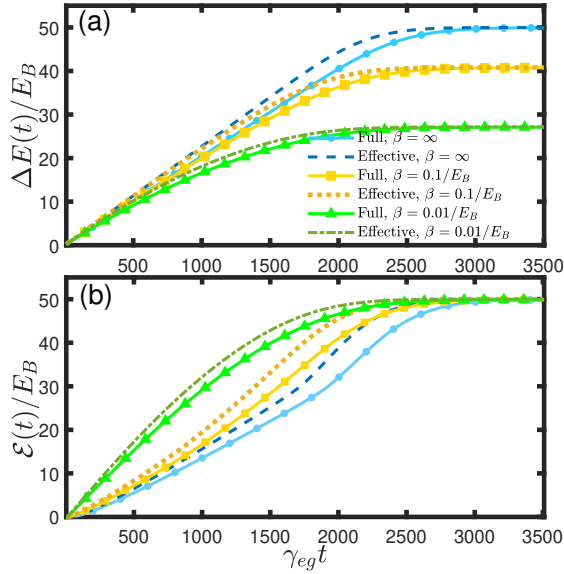


FIG. 4. Charging performance in the presence of the decay from $|h\rangle$ to $|e\rangle$ with $\gamma_{he} = \gamma_{eg}$ under various inverse temperature β ($k_B \equiv 1$). (a) Energy stored in the battery $\Delta E(t)$. (b) Ergotropy $\mathcal{E}(t)$. The driving intensity is fixed as $\Omega = 0.05\gamma_{hg}$. Other parameters are the same as in Fig. 3.

respectively. $\beta = \infty$ means the ground state. It can be found that both energy and ergotropy still monotonically increase with the charging time and ultimately stabilise with their respective maximum values. Note high-ergotropy state is different from high-energy state in population distribution. Due to the unidirectional transition from the lower Fock states to the higher ones as indicated in Eq. (10b), an initially higher-temperature battery state is more convenient to be transformed to be a higher-ergotropy state than the lower-temperature state. The final increment of ΔE for an initially high-temperature state is significantly smaller than that for $\mathcal{E}(t)$. Moreover, we take account of a nonvanishing γ_{he} in Fig. 4. In comparison to Fig. 3, one can find that the effect of the process shown in Fig. 2(b) is marginal in the charging efficiency, that is consistent with our analysis.

IV. LARGE SPIN BATTERY

To implement our charging scheme in a more physically relevant scenario, we consider an $N = 2J+1$ dimensional large-spin battery in this section. The battery Hamiltonian reads $H_B = E_B J_z = E_B \sum_{m=-J}^J m |J, m\rangle \langle J, m|$, where J is an integer or half-integer quantum number of energy. The charger and the battery interact with each other through

$$H_I = g(J_+ |e\rangle \langle h| + J_- |h\rangle \langle e|), \quad (20)$$

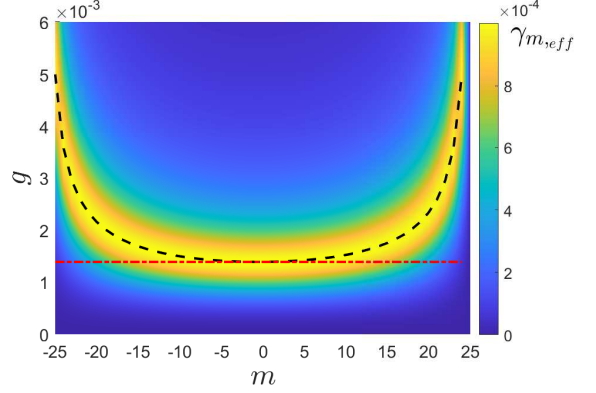


FIG. 5. Effective transition rate $\gamma_{m,\text{eff}}$ (in unit of E_B) from $|J, m\rangle$ to $|J, m+1\rangle$ in the parameter space of g (in unit of E_B) and m . The black dashed line indicates the optimization condition in Eq. (23). The horizontal red dot-dashed line indicates the optimization condition for $m = 0$. The energy quantum number is set as $J = 25$. The driving intensity is $\Omega = 0.1\gamma_{hg}$. The other parameters are the same as in Fig. 3.

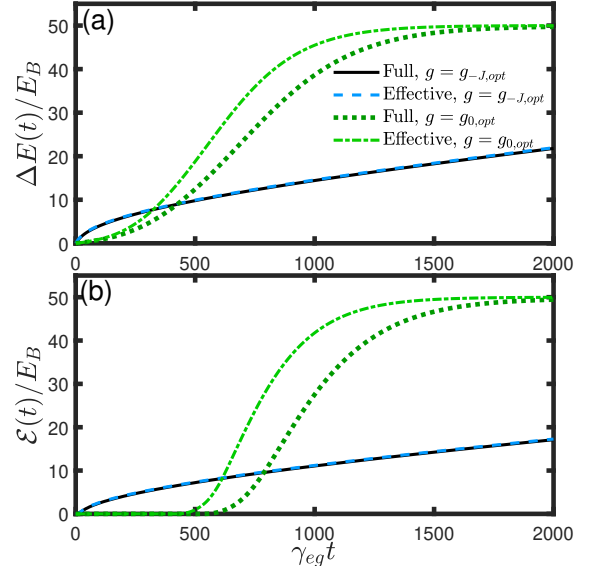


FIG. 6. Full and effective dynamics of (a) battery energy $\Delta E(t)$ and (b) ergotropy $\mathcal{E}(t)$ as functions of $\gamma_{eg}t$ under the optimization conditions of $g = g_{m=-J,\text{opt}}$ (solid lines and dashed lines) and $g = g_{m=0,\text{opt}}$ (dotted lines and dot-dashed line), as defined in Eq. (23). The quantum number of energy is set as $J = 25$ and the decay rate is $\gamma_{he} = \gamma_{eg}$. $\Omega = 0.1\gamma_{hg}$. The other parameters are the same as in Fig. 3.

where the creation operator of battery is the collective angular momentum operator

$$J_+ = \sum_{m=-J}^J \sqrt{J(J+1) - m(m+1)} |J, m+1\rangle \langle J, m|, \quad (21)$$

and $J_- = J_+^\dagger$. The effective transition rate from $|J, m\rangle$ to $|J, m+1\rangle$ can be obtained by substituting $A_m =$

$\sqrt{J(J+1) - m(m+1)}$ to Eq. (14). We have

$$\gamma_{m,\text{eff}} = \left| \frac{\sqrt{\gamma_{eg}}\Omega g \sqrt{J(J+1) - m(m+1)}}{g^2[J(J+1) - m(m+1)] - \tilde{\Delta}\tilde{\delta}} \right|^2. \quad (22)$$

In contrast to the uniform model with $A_n = 1$, the effective transition rates in the large spin model vary across different subspaces, the same is true for the optimization condition:

$$g_{m,\text{opt}}^2[J(J+1) - m(m+1)] = |\tilde{\Delta}\tilde{\delta}|. \quad (23)$$

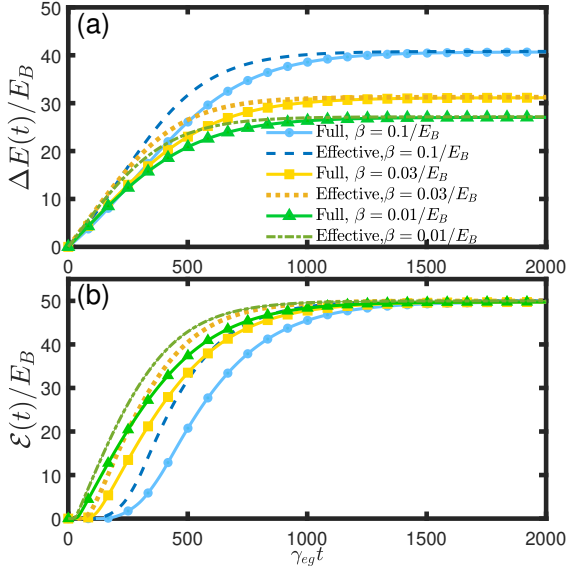


FIG. 7. Full and effective dynamics of (a) energy stored in the battery $\Delta E(t)$ and (b) ergotropy $\mathcal{E}(t)$ as functions of $\gamma_{eg}t$ under initial thermal states with different inverse temperature β . The other parameters are the same as in Fig. 6.

In Fig. 5, we present the dependence of effective transition rate $\gamma_{m,\text{eff}}$ on the coupling strength between the qutrit charger and the large-spin battery g and the quantum number of angular momentum m to confirm the optimization condition in Eq. (23), as indicated by the black dashed line. It is noted that by setting $m = 0$ in Eq. (23), the relevant $\gamma_{m,\text{eff}}$ closely approximates the optimal conditions across a substantial number of subspaces as shown by the red dash-dotted line. In practice, it is a m -independent setting for enhancing the charging efficiency.

In Fig. 6(a) and 6(b), we compare the charging efficiency under the optimized condition of $g = g_{m=-J,\text{opt}}$ with that under $g = g_{m=0,\text{opt}}$ when the battery is initialised as the ground state $\rho_B(0) = |J, -J\rangle\langle J, -J|$. It is found that while the optimized condition $g = g_{-J,\text{opt}}$ exhibits an advantage at the beginning of charging due to the initial population distribution, the charging rate under $g = g_{0,\text{opt}}$ dramatically increases as the charging proceeds. The latter quickly surpasses the former. This

behavior is consistent with our effective master equation. Nevertheless, the effective dynamics under $g = g_{0,\text{opt}}$ exhibits a moderate deviation from the full one, and it perfectly matches with the full dynamics under $g = g_{-J,\text{opt}}$.

Now we check the case that the large-spin battery is initially prepared at the thermal states with various inverse temperature β by the dynamics of stored energy $\Delta E(t)$ and ergotropy $\mathcal{E}(t)$ in Fig. 7(a) and 7(b), respectively. The optimization condition is chosen as $g = g_{0,\text{opt}}$. It is found that the ergotropy can be maintained about $\mathcal{E}_{\text{steady}} > 0.995\mathcal{E}_{\text{max}}$, irrespective to the temperature β of the initial state, where $\mathcal{E}_{\text{max}} = 2JE_B$. Moreover, it is interesting to find that a higher initial temperature of the battery results in a higher growth rate of the ergotropy.

V. HARMONIC OSCILLATOR BATTERY

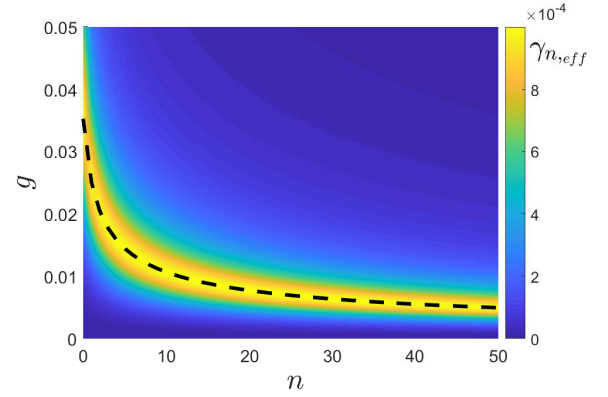


FIG. 8. Effective transition rate $\gamma_{n,\text{eff}}$ (in unit of E_B) from $|n\rangle$ to $|n+1\rangle$ in the parametric space of g (in unit of E_B) and n . The black dashed line indicates the optimization condition in Eq. (25). The battery size is chosen as $N = 50$. $\Omega = 0.1\gamma_{hg}$. The other parameters are the same as in Fig. 3.

In this section, we consider a quantum battery consisting of an $N + 1$ -dimensional truncated harmonic oscillator. In this case, the ladder operator becomes a truncated bosonic creation operator $A^\dagger = \sum_{n=0}^{N-1} \sqrt{n+1}|n+1\rangle\langle n|$. The effective transition rate from $|n\rangle$ to $|n+1\rangle$ can be obtained by substituting $A_n = \sqrt{n+1}$ to Eq. (14):

$$\gamma_{n,\text{eff}} = \left| \frac{\sqrt{\gamma_{eg}}\Omega g \sqrt{n+1}}{g^2(n+1) - \tilde{\Delta}\tilde{\delta}} \right|^2. \quad (24)$$

Subsequently, it can be optimized under the condition

$$g_{n,\text{opt}}^2(n+1) = |\tilde{\Delta}\tilde{\delta}|. \quad (25)$$

The effective transition rate in the parameter space of charger-battery coupling strength g and n is plotted in Fig. 8. The optimization condition is indicated by the black dashed line. Distinct from the large-spin battery, it is hardly to find a subspace-independent coupling strength g_{opt} to optimize the effective transition rates

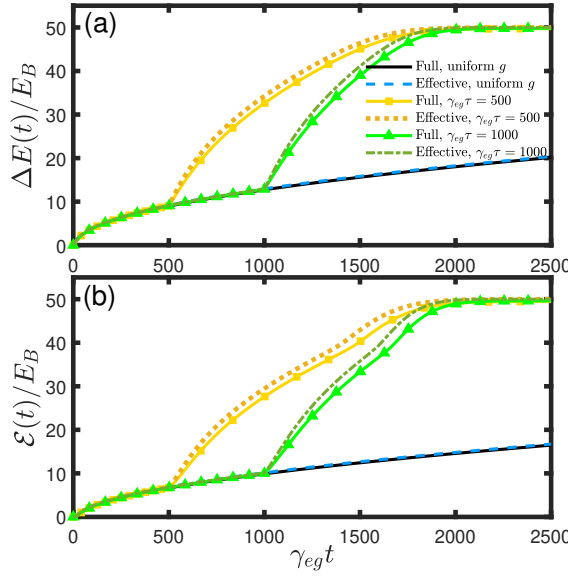


FIG. 9. Full and effective dynamics of (a) battery energy $\Delta E(t)$ and (b) ergotropy $\mathcal{E}(t)$ as functions of $\gamma_{eg}t$ with an invariant coupling strength $g = g_{0,\text{opt}}$ in Eq. (25) during the charging process (black solid lines and blue dashed lines) and with a coupling strength quenched at $\gamma_{eg}\tau$ (green and yellow lines) according to Eq. (26). The decay rate $\gamma_{he} = \gamma_{eg}$. $\Omega = 0.1\gamma_{hg}$. The other parameters are the same as in Fig. 3.

for the harmonic-oscillator battery, since $g_{n,\text{opt}}$ decreases with n in a monotonic way. Nevertheless, the charging efficiency can be enhanced by adjusting the coupling strength during the charging process. By our scheme, one can initially optimize the effective transition rate from $|0\rangle$ to $|1\rangle$ by choosing $g = g_{0,\text{opt}}$ in Eq. (25) due to the fact that the ground state is always the most populated state for a thermal state. Then after an interval of τ , one can modify the coupling strength to be

$$g = g_{\bar{n}(\tau),\text{opt}} = \sqrt{\frac{|\tilde{\Delta}\delta|}{\bar{n}(\tau) + 1}}, \quad (26)$$

where $\bar{n}(\tau) = \text{Tr}[\rho_B(\tau)H_B]/E_B$ is the instantaneous average excitation of the truncated HO battery.

We compare the charging performance with a uniform g during the whole charging evolution and that with a quenched g by the dynamics of $\Delta E(t)$ and $\mathcal{E}(t)$ in Figs. 9(a) and 9(b), respectively. The yellow and green lines indicate the quenched moment at $\gamma_{eg}\tau = 500$ and $\gamma_{eg}\tau = 1000$, respectively, in which the charger-battery coupling strength is only modified at the specified moment and calculated according to Eq. (26). The battery is initially prepared in the ground state $\rho_B(0) = |0\rangle\langle 0|$. It is clearly that the strategy of a uniform g is the lowest in charging efficiency and both energy and ergotropy have an abrupt and significant enhancement when g can be re-optimized. The numerical simulation indicates that the full dynamics is perfectly matched with the effective

dynamics and the charging efficiency is slightly overestimated after the adjustment of the coupling strength g .

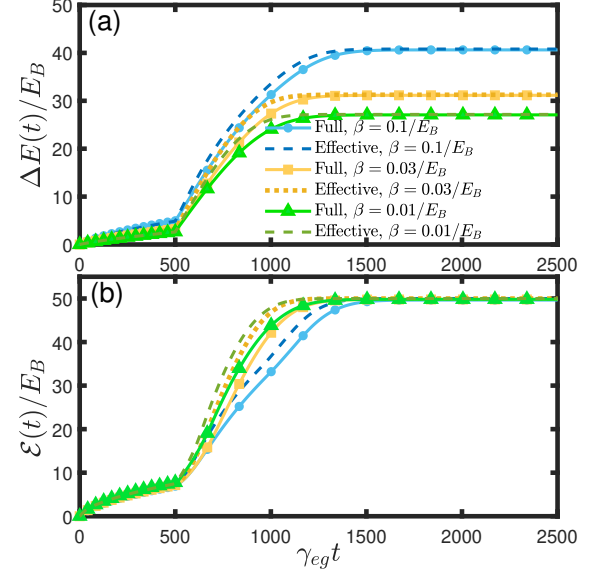


FIG. 10. Full and effective dynamics of (a) energy stored in the battery $\Delta E(t)$ and (b) ergotropy $\mathcal{E}(t)$ as functions of $\gamma_{eg}t$ under initial thermal states with various β . The coupling strength is only modified at $\gamma_{eg}\tau = 500$ according to Eq. (26). The other parameters are the same as in Fig. 9.

The dynamics of the stored energy $\Delta E(t)$ and ergotropy $\mathcal{E}(t)$ for charging the HO battery initially in the thermal states with a finite temperature is demonstrated in Figs. 10(a) and 10(b), respectively. The results are similar to the large-spin battery presented in Fig. 7. A higher initial temperature or energy results in a higher growth rate of the ergotropy. In addition, the steady value of the ergotropy is insensitive to the initial inverse temperature β . In this case, we have $\mathcal{E}_{\text{steady}} > 0.994\mathcal{E}_{\text{max}}$ with $\mathcal{E}_{\text{max}} = NE_B$.

VI. CONCLUSION

In summary, we have proposed a stable charging scheme assisted by a dissipative Δ -type qutrit, which relies on the nonreciprocal interaction between the external power source and the battery and the ensued unidirectional energy flow. Three types of finite dimensional quantum batteries, including the uniform coupling strength model, the large-spin battery, and the truncated harmonic oscillator battery, have confirmed that the battery energy and ergotropy can be maintained at their respective maximum values and the battery need not to be decoupled from the charger after the charging process is completed. By deriving the effective master equation of the battery, we can obtain the optimization condition of the charging efficiency. For the large spin battery, the charging efficiency can be significantly en-

hanced by choosing the charger-battery coupling strength according to the optimization condition in the subspace with $m = 0$. For the truncated harmonic oscillator battery, the enhancement can be achieved by adjusting the coupling strength according to the instantaneous state of the battery during charging. In application, our work provides an efficient initial-state-independent charging scheme and avoids the discharging induced by the time-reversal symmetry. In theory, it extends the high-order Fermi's Golden rule to the regime of non-Hermitian Hamiltonian.

Appendix A: The effective master equation

This appendix contributes to deriving the effective Hamiltonian and Lindblad operators for the quantum battery $\rho_B(t)$ using a technique extending the James' method [49–51] from Hamiltonian to Lindbladian.

By defining a non-Hermitian Hamiltonian

$$H_{\text{NH}} = H' - \frac{i}{2} \sum_{k=hg,eg,he} L_k^\dagger L_k = \tilde{H} + V, \quad (\text{A1})$$

$$\tilde{H} = \tilde{\Delta} |h\rangle\langle h| + \tilde{\delta} |e\rangle\langle e| + g(A^\dagger |e\rangle\langle h| + \text{H.c.}), \quad (\text{A2})$$

$$V = \Omega |h\rangle\langle g| + \text{H.c.}, \quad (\text{A3})$$

where L_{hg} , L_{eg} , and L_{he} are $\sqrt{\gamma_{hg}}|g\rangle\langle h|$, $\sqrt{\gamma_{eg}}|g\rangle\langle e|$, and $\sqrt{\gamma_{he}}|h\rangle\langle e|$, respectively, and $\tilde{\Delta} = \Delta - i\gamma_{hg}/2 - i\gamma_{he}/2$ and $\tilde{\delta} = \delta - i\gamma_{eg}/2$ are complex detunings, the full master equation (4) can be rewritten as

$$\dot{\rho}(t) = -i[(\tilde{H} + V)\rho(t) - \rho(t)(\tilde{H}^\dagger + V)] + L_{hg}\rho(t)L_{hg}^\dagger + L_{eg}\rho(t)L_{eg}^\dagger + L_{he}\rho(t)L_{he}^\dagger. \quad (\text{A4})$$

In the weak-driving regime [52], the subspace spanned by $\{|gn\rangle, |hn\rangle, |e(n+1)\rangle, |g(n+1)\rangle\}$ with $n < N$ in Fig. 2(a) can be divided into the rapidly-decaying excited subspace spanned by $\{|hn\rangle, |e(n+1)\rangle\}$ and the ground subspace spanned by $\{|gn\rangle, |g(n+1)\rangle\}$. With respect to Fig. 2(a), the non-Hermitian Hamiltonian defined in Eq. (A2) is given by

$$\tilde{H}_n = \tilde{\Delta} |hn\rangle\langle hn| + \tilde{\delta} |e(n+1)\rangle\langle e(n+1)| + gA_n [|hn\rangle\langle e(n+1)| + |e(n+1)\rangle\langle hn|], \quad (\text{A5})$$

involving only with the excited subspaces. The weak external driving V leads to the excitation process from the ground subspaces to the excited subspaces with a Hermitian Hamiltonian

$$V_n = V_{+,n} + V_{+,n}^\dagger = \Omega |hn\rangle\langle gn| + \text{H.c.} \quad (\text{A6})$$

The Lindblad operators induced by the qutrit decay read

$$\begin{aligned} L_{hg,n} &= \sqrt{\gamma_{hg}}|gn\rangle\langle hn|, \\ L_{eg,n} &= \sqrt{\gamma_{eg}}|g(n+1)\rangle\langle e(n+1)|. \end{aligned} \quad (\text{A7})$$

To employ the perturbation theory, it is convenient to transform to the rotating frame with respect to $\tilde{U}(t) =$

$e^{i\tilde{H}t}$. The master equation (A4) then becomes

$$\begin{aligned} \dot{\tilde{\rho}}(t) &= -i[\tilde{V}(t)\tilde{\rho}(t) - \tilde{\rho}(t)\tilde{V}^\dagger(t)] + \tilde{L}_{hg}(t)\tilde{\rho}(t)\tilde{L}_{hg}^\dagger(t) \\ &\quad + \tilde{L}_{eg}(t)\tilde{\rho}(t)\tilde{L}_{eg}^\dagger(t) + \tilde{L}_{he}(t)\tilde{\rho}(t)\tilde{L}_{he}^\dagger(t), \end{aligned} \quad (\text{A8})$$

where $\tilde{\rho}(t) = \tilde{U}(t)\rho(t)\tilde{U}^\dagger(t)$ is the density matrix in the rotating frame. The other operators are transformed accordingly with $\tilde{\mathcal{O}}(t) = \tilde{U}(t)\mathcal{O}\tilde{U}^{-1}(t)$, $\mathcal{O} = V$, L_{hg} , L_{eg} , and L_{he} .

With respect to the main process in Fig. 2(a), the transformed master equation (A8) in the subspace can be written as

$$\begin{aligned} \dot{\tilde{\rho}}_n(t) &= -i[\tilde{V}_n(t)\tilde{\rho}_n(t) - \tilde{\rho}_n(t)\tilde{V}_n^\dagger] \\ &\quad + \tilde{L}_{hg,n}(t)\tilde{\rho}_n(t)\tilde{L}_{hg,n}^\dagger(t) \\ &\quad + \tilde{L}_{eg,n}(t)\tilde{\rho}_n(t)\tilde{L}_{eg,n}^\dagger(t), \end{aligned} \quad (\text{A9})$$

where

$$\tilde{V}_n(t) = \Omega(e^{i\tilde{H}_n t} |hn\rangle\langle gn| + |gn\rangle\langle hn|e^{-i\tilde{H}_n t}), \quad (\text{A10})$$

$$\tilde{L}_{hg,n}(t) = \sqrt{\gamma_{hg}}|gn\rangle\langle hn|e^{-i\tilde{H}_n t}, \quad (\text{A11})$$

$$\tilde{L}_{eg,n}(t) = \sqrt{\gamma_{eg}}|g(n+1)\rangle\langle e(n+1)|e^{-i\tilde{H}_n t}. \quad (\text{A12})$$

The last term about $\tilde{L}_{he}(t)$ in Eq. (A8) that appears only as the leading-order contribution depicted in Fig. 2(b) will be analyzed later.

Then we vectorize the density matrix of each subspace to be a $4^2 \times 1$ vector denoted by $|\tilde{\rho}_n(t)\rangle\rangle$. The equation of motion in this representation is given by

$$\partial_t |\tilde{\rho}_n(t)\rangle\rangle = \mathbf{L}_n(t) |\tilde{\rho}_n(t)\rangle\rangle. \quad (\text{A13})$$

Her, $\mathbf{L}(t)$ is the $4^2 \times 4^2$ superoperator in the form of

$$\begin{aligned} \mathbf{L}_n(t) &= \mathcal{V}_n(t) + \mathcal{J}_n(t), \\ \mathcal{V}_n(t) &= -i(\mathbb{I} \otimes \tilde{V}_n(t) - \tilde{V}_n^*(t) \otimes \mathbb{I}), \\ \mathcal{J}_n(t) &= \tilde{L}_{hg,n}^*(t) \otimes \tilde{L}_{hg,n}(t) + \tilde{L}_{eg,n}^*(t) \otimes \tilde{L}_{eg,n}(t), \end{aligned} \quad (\text{A14})$$

where \mathbb{I} is the 4×4 identity operator in the subspace [53]. $\mathcal{V}(t)$ and $\mathcal{J}(t)$ represent the non-Hermitian evolution part and the quantum jump part, respectively. The formal solution of Eq. (A13) is

$$|\tilde{\rho}_n(t)\rangle\rangle = |\tilde{\rho}_n(0)\rangle\rangle + \int_0^t dt_1 \mathbf{L}_n(t_1) |\tilde{\rho}_n(t_1)\rangle\rangle. \quad (\text{A15})$$

In the large detuning condition, i.e., $\Delta + \delta \gg \Omega$, the transformation operator $U(t) = e^{iH_n(t)} \propto \exp[i(\tilde{\Delta} + \tilde{\delta})t/2]$ is highly oscillating with time. By iteratively substituting Eq. (A15) into Eq. (A13), neglecting the fast oscillating terms $\mathcal{V}(t)|\tilde{\rho}_n(0)\rangle\rangle$, and taking the Markovian approximation [51], the equation of motion can written into a Dyson series:

$$\begin{aligned}\partial_t |\tilde{\rho}_n(t)\rangle\rangle &= \left[\mathbf{L}_n(t) \int_0^t dt_1 \mathbf{L}_n(t_1) + \mathbf{L}_n(t) \int_0^t dt_1 \mathbf{L}_n(t_1) \int_0^{t_1} dt_2 \mathbf{L}_n(t_2) + \dots \right] |\tilde{\rho}_n(t)\rangle\rangle. \\ &= \left[\mathbf{L}_{\text{eff},n}^{(2)}(t) + \mathbf{L}_{\text{eff},n}^{(3)}(t) + \dots \right] |\tilde{\rho}_n(t)\rangle\rangle.\end{aligned}\quad (\text{A16})$$

It is assumed that the qutrit remains mostly in its ground state during the charging process $|\tilde{\rho}(t)\rangle\rangle \approx \mathcal{P}_g |\tilde{\rho}(t)\rangle\rangle$, where $\mathcal{P}_g = P_g \otimes P_g$. The equation of motion for the ground-state branch then takes the form

$$\begin{aligned}\partial_t \mathcal{P}_g |\tilde{\rho}_n(t)\rangle\rangle &\approx \mathcal{P}_g \left[\mathbf{L}_{\text{eff},n}^{(2)}(t) + \mathbf{L}_{\text{eff},n}^{(3)}(t) \right] \mathcal{P}_g |\tilde{\rho}_n(t)\rangle\rangle \\ &= \mathcal{P}_g \left[\mathcal{V}_n(t) \int_0^t dt_1 \mathcal{V}_n(t_1) \right. \\ &\quad \left. + \mathcal{J}_n(t) \int_0^t dt_1 \mathcal{V}_n(t_1) \int_0^{t_1} dt_2 \mathcal{V}_n(t_2) \right] \mathcal{P}_g |\tilde{\rho}_n(t)\rangle\rangle.\end{aligned}\quad (\text{A17})$$

up to the second order in driving intensity Ω . By substituting Eq. (A10) into the first term of the Eq. (A17), we can obtain the effective superoperator for a non-Hermitian evolution:

$$\begin{aligned}\mathcal{P}_g \mathcal{V}_n(t) \int_0^t dt_1 \mathcal{V}_n(t_1) \mathcal{P}_g \\ = - \left[P_g \otimes V_{+,n}^\dagger (i\tilde{H}_n)^{-1} V_{+,n} + V_{+,n}^\dagger (-i\tilde{H}_n^*)^{-1} V_{+,n} \otimes P_g \right],\end{aligned}\quad (\text{A18})$$

where we used the identity $\int dt e^{i\tilde{H}t} = (i\tilde{H})^{-1} e^{i\tilde{H}t}$. In the original representation for density matrix, it corresponds to the non-Hermitian effective Hamiltonian

$$\mathcal{H}_n^{\text{eff}} = -V_{+,n}^\dagger (\tilde{H}_n)^{-1} V_{+,n} = -\frac{\Omega^2 \tilde{\delta}}{\tilde{\Delta} \tilde{\delta} - g^2 A_n^2} |gn\rangle\langle gn|.\quad (\text{A19})$$

By substituting Eqs. (A10)-(A12) into the second term of Eq. (A17), we can obtain the effective superoperator for quantum jumps:

$$\begin{aligned}\mathcal{P}_g \mathcal{J}_n(t) \int_0^t dt_1 \mathcal{V}_n(t_1) \int_0^{t_1} dt_2 \mathcal{V}_n(t_2) \mathcal{P}_g \\ = L_{hg,n} (\tilde{H}_n^*)^{-1} V_{+,n} \otimes L_{hg,n} (\tilde{H}_n)^{-1} V_{+,n} \\ + L_{eg,n} (\tilde{H}_n^*)^{-1} V_{+,n} \otimes L_{eg,n} (\tilde{H}_n)^{-1} V_{+,n}.\end{aligned}\quad (\text{A20})$$

By transforming back to the original representation, the second-order effective Lindblad operators turn out to be

$$L_{hg,n}^{\text{eff}} = L_{hg,n} (\tilde{H}_n)^{-1} V_{+,n} = \frac{\sqrt{\gamma_{hg}} \Omega \tilde{\delta}}{\tilde{\Delta} \tilde{\delta} - g^2 A_n^2} |gn\rangle\langle gn|,\quad (\text{A21})$$

$$L_{eg,n}^{\text{eff}} = L_{eg,n} (\tilde{H}_n)^{-1} V_{+,n} = \frac{\sqrt{\gamma_{eg}} \Omega g A_n}{g^2 A_n^2 - \tilde{\Delta} \tilde{\delta}} |g(n+1)\rangle\langle gn|.\quad (\text{A22})$$

Therefore according to Eq. (A17), the equation of motion

in the ground state subspaces reads

$$\begin{aligned}P_g \dot{\rho}_n(t) P_g &= -i \left[\mathcal{H}_n^{\text{eff}} \rho_n(t) - \rho_n(t) (\mathcal{H}_n^{\text{eff}})^\dagger \right] \\ &\quad + L_{hg,n}^{\text{eff}} \rho(t) (L_{hg,n}^{\text{eff}})^\dagger + L_{eg,n}^{\text{eff}} \rho(t) (L_{eg,n}^{\text{eff}})^\dagger.\end{aligned}\quad (\text{A23})$$

It can be rewritten as a standard master equation

$$\begin{aligned}P_g \dot{\rho}_n(t) P_g &= -i \left[H_n^{\text{eff}}, \rho_n(t) \right] + \mathcal{L}[L_{hg,n}^{\text{eff}}] \rho_n(t) \\ &\quad + \mathcal{L}[L_{eg,n}^{\text{eff}}] \rho_n(t)\end{aligned}\quad (\text{A24})$$

with a Hermitian effective Hamiltonian

$$H_n^{\text{eff}} = -\Omega^2 \text{Re} \left[\frac{\tilde{\delta}}{\tilde{\Delta} \tilde{\delta} - g^2 A_n^2} \right] |gn\rangle\langle gn|.\quad (\text{A25})$$

It is the Hermitian part of the operator

$$\begin{aligned}h_n^{\text{eff}} &= \mathcal{H}_n^{\text{eff}} + \frac{i}{2} \sum_{k=hg,eg} (L_{k,n}^{\text{eff}})^\dagger L_{k,n}^{\text{eff}} \\ &= \mathcal{H}_n^{\text{eff}} + \frac{i}{2} V_{+,n}^\dagger (\tilde{H}_n^\dagger)^{-1} \sum_{k=hg,eg,he} L_{k,n}^\dagger L_{k,n} \tilde{H}_n^{-1} V_{+,n} \\ &\quad - \frac{i}{2} V_{+,n}^\dagger (\tilde{H}_n^\dagger)^{-1} L_{he,n}^\dagger L_{he,n} \tilde{H}_n^{-1} V_{+,n} \\ &= \mathcal{H}_n^{\text{eff}} + \frac{1}{2} V_{+,n}^\dagger (\tilde{H}_n^\dagger)^{-1} \left(\tilde{H}_n^\dagger - \tilde{H}_n \right) \tilde{H}_n^{-1} V_{+,n} \\ &\quad - \frac{i}{2} V_{+,n}^\dagger (\tilde{H}_n^\dagger)^{-1} L_{he,n}^\dagger L_{he,n} \tilde{H}_n^{-1} V_{+,n} \\ &= \mathcal{H}_n^{\text{eff}} - \frac{1}{2} V_{+,n}^\dagger \left[(\tilde{H}_n^\dagger)^{-1} - \tilde{H}_n^{-1} \right] V_{+,n} - \frac{i}{2} (L_{he,n}^{\text{eff}})^\dagger L_{he,n}^{\text{eff}} \\ &= H_n^{\text{eff}} - \frac{i}{2} (L_{he,n}^{\text{eff}})^\dagger L_{he,n}^{\text{eff}},\end{aligned}\quad (\text{A26})$$

where $L_{he,n} = \sqrt{\gamma_{he}} |en\rangle\langle hn|$. The non-Hermitian part represents the leakage from $|gn\rangle$ to $|en\rangle$ with the jump operator $L_{he,n}^{\text{eff}} = L_{he,n} \tilde{H}_n^{-1} V_{+,n}$. It is negligible comparing to the spontaneous decay γ_{eg} under the condition $\Delta, \gamma_{hg} \gg \gamma_{he}, \Omega$.

For the uppermost ground-state subspace spanned by $\{|gN\rangle, |hN\rangle\}$, the non-Hermitian Hamiltonian reads

$$\tilde{H}_N = \tilde{\Delta} |hN\rangle\langle hN|.\quad (\text{A27})$$

Following the same procedure, the effective Lindblad operator and the effective Hamiltonian turn out to be

$$L_{hg,N}^{\text{eff}} = L_{hg,N} \tilde{H}_N V_{+,N} = \frac{\sqrt{\gamma_{hg}} \Omega}{\tilde{\Delta}} |gN\rangle\langle gN|,\quad (\text{A28})$$

$$H_N^{\text{eff}} = -\Omega^2 \text{Re} \left(\frac{1}{\tilde{\Delta}} \right) |gN\rangle\langle gN|,\quad (\text{A29})$$

respectively. Up to this point, we have established the effective master equation describing the main unidirectional charging mechanism in Fig. 2(a).

The leading-order correction induced by the decay γ_{he} is described in Fig. 2(b). The process $|gn\rangle \rightarrow |hn\rangle \rightarrow |en\rangle \rightarrow |gn\rangle$ gives rise to a pure dephasing effect on $|gn\rangle$, which is associated with a higher order term $\mathbf{L}_{\text{eff},n}^{(4)}$ in Eq. (A16)

$$J_{eg,n}^{\text{eff}*} \otimes J_{eg,n}^{\text{eff}} = \mathcal{P}_g \tilde{L}_{eg,n-1}^*(t) \otimes \tilde{L}_{eg,n-1}(t) \int_0^t dt_1 \mathcal{J}_{he,n}(t_1) \times \int_0^{t_1} dt_2 \mathcal{V}_n(t_2) \int_0^{t_2} dt_3 \mathcal{V}_n(t_3) \mathcal{P}_g, \quad (\text{A30})$$

where $\mathcal{J}_{he,n}(t)$ describes the decay γ_{he} :

$$\mathcal{J}_{he,n}(t) = e^{-i\tilde{H}_{n-1}^* t} L_{he,n} e^{i\tilde{H}_n^* t} \otimes e^{i\tilde{H}_{n-1} t} L_{he,n} e^{-i\tilde{H}_n t} \quad (\text{A31})$$

with $L_{he,n} = \sqrt{\gamma_{he}} |en\rangle \langle hn|$. The dephasing rate turns out to be

$$\frac{|\langle gn | J_{eg,n}^{\text{eff}} | gn \rangle|^2}{|\langle gn | L_{hg,n}^{\text{eff}} | gn \rangle|^2} = \frac{\gamma_{eg} \gamma_{he}}{\gamma_{hg}} \mathbf{H}_{en,en}^{-1}, \quad (\text{A32})$$

where $\mathbf{H}_{en,en}^{-1}$ is defined as

$$\mathbf{H}_{en,en}^{-1} = \langle en | \otimes \langle en | \times \left(-i\tilde{H}_{n-1}^* \otimes \mathbb{I} + \mathbb{I} \otimes i\tilde{H}_{n-1} \right)^{-1} | en \rangle \otimes | en \rangle \quad (\text{A33})$$

using the identity $e^{-i\tilde{H}^* t} \otimes e^{i\tilde{H} t} = \exp(-i\tilde{H}^* t \otimes \mathbb{I} + \mathbb{I} \otimes$

$i\tilde{H} t)$. Similarly, the process $|gn\rangle \rightarrow |hn\rangle \rightarrow |en\rangle \rightarrow |h(n-1)\rangle \rightarrow |g(n-1)\rangle$ in Fig. 2(b) gives rise to an effective transition from $|gn\rangle$ to $|g(n-1)\rangle$, the relevant jump superoperator is given by

$$J_{hg,n}^{\text{eff}*} \otimes J_{hg,n}^{\text{eff}} = \mathcal{P}_g \tilde{L}_{hg,n-1}^*(t) \otimes \tilde{L}_{hg,n-1}(t) \times \int_0^t dt_1 \mathcal{J}_{he,n}(t_1) \int_0^{t_1} dt_2 \mathcal{V}_n(t_2) \int_0^{t_2} dt_3 \mathcal{V}_n(t_3) \mathcal{P}_g. \quad (\text{A34})$$

The ratio of the effective decay rate from $|gn\rangle$ to $|g(n-1)\rangle$ in Fig. 2(b) to that from $|gn\rangle$ to $|g(n+1)\rangle$ in Fig. 2(a) is

$$\frac{|\langle g(n-1) | J_{hg,n}^{\text{eff}} | gn \rangle|^2}{|\langle g(n+1) | L_{eg,n}^{\text{eff}} | gn \rangle|^2} = \frac{\gamma_{hg} \gamma_{he} |\tilde{\delta}|^2}{\gamma_{eg} g^2 A_n^2} \mathbf{H}_{h(n-1),en}^{-1}, \quad (\text{A35})$$

where $\mathbf{H}_{g(n-1),en}^{-1}$ is given by

$$\mathbf{H}_{h(n-1),en}^{-1} = \langle h(n-1) | \otimes \langle h(n-1) | \times \left(-i\tilde{H}_{n-1}^* \otimes \mathbb{I} + \mathbb{I} \otimes i\tilde{H}_{n-1} \right)^{-1} | en \rangle \otimes | en \rangle. \quad (\text{A36})$$

Under the parametric settings that $\gamma_{eg} \approx \gamma_{he} \ll \gamma_{hg}$, it is important to observe that the dephasing rate given by Eq. (A32) is negligible in comparison to that in Eq. (A21). Similarly, the effective transition rate from $|gn\rangle$ to $|g(n-1)\rangle$ given by Eq. (A35) is negligible in comparison to that from $|gn\rangle$ to $|g(n+1)\rangle$ in Eq. (A22) under the condition $\gamma_{eg} \approx \gamma_{he} \ll \gamma_{hg}$ and $\Delta \gg \delta$ due to our optimization condition $g^2 A_n^2 \approx |\tilde{\Delta}\tilde{\delta}|$.

[1] F. Campaioli, S. Gherardini, J. Q. Quach, M. Polini, and G. M. Andolina, *Colloquium: Quantum batteries*, *Rev. Mod. Phys.* **96**, 031001 (2024).

[2] A. Auffèves, *Quantum technologies need a quantum energy initiative*, *PRX Quantum* **3**, 020101 (2022).

[3] M. Horodecki and J. Oppenheim, *Fundamental limitations for quantum and nanoscale thermodynamics*, *Nat. Commun.* **4**, 2059 (2013).

[4] K. V. Hovhannisyan, M. Perarnau-Llobet, M. Huber, and A. Acín, *Entanglement generation is not necessary for optimal work extraction*, *Phys. Rev. Lett.* **111**, 240401 (2013).

[5] S. Vinjanampathy and J. Anders, *Quantum thermodynamics*, *Contemp. Phys.* **57**, 545 (2016).

[6] F. Campaioli, F. A. Pollock, and S. Vinjanampathy, *Quantum batteries*, in *Thermodynamics in the Quantum Regime: Fundamental Aspects and New Directions*, edited by F. Binder, L. A. Correa, C. Gogolin, J. Anders, and G. Adesso (Springer International Publishing, Cham, 2018) pp. 207–225.

[7] R. Alicki and M. Fannes, *Entanglement boost for extractable work from ensembles of quantum batteries*, *Phys. Rev. E* **87**, 042123 (2013).

[8] F. Campaioli, F. A. Pollock, F. C. Binder, L. Céleri, J. Goold, S. Vinjanampathy, and K. Modi, *Enhancing the charging power of quantum batteries*, *Phys. Rev. Lett.* **118**, 150601 (2017).

[9] F. H. Kamin, F. T. Tabesh, S. Salimi, and A. C. Santos, *Entanglement, coherence, and charging process of quantum batteries*, *Phys. Rev. E* **102**, 052109 (2020).

[10] G. M. Andolina, M. Keck, A. Mari, M. Campisi, V. Giovannetti, and M. Polini, *Extractable work, the role of correlations, and asymptotic freedom in quantum batteries*, *Phys. Rev. Lett.* **122**, 047702 (2019).

[11] S. Seah, M. Perarnau-Llobet, G. Haack, N. Brunner, and S. Nimmrichter, *Quantum speed-up in collisional battery charging*, *Phys. Rev. Lett.* **127**, 100601 (2021).

[12] M. B. Arjmandi, A. Shokri, E. Faizi, and H. Mohammadi, *Performance of quantum batteries with correlated and uncorrelated chargers*, *Phys. Rev. A* **106**, 062609 (2022).

[13] H.-L. Shi, S. Ding, Q.-K. Wan, X.-H. Wang, and W.-L. Yang, *Entanglement, coherence, and extractable work in quantum batteries*, *Phys. Rev. Lett.* **129**, 130602 (2022).

[14] D.-L. Yang, F.-M. Yang, and F.-Q. Dou, *Three-level dicke quantum battery*, *Phys. Rev. B* **109**, 235432 (2024).

[15] D. Ferraro, M. Campisi, G. M. Andolina, V. Pel

legrini, and M. Polini, *High-power collective charging of a solid-state quantum battery*, *Phys. Rev. Lett.* **120**, 117702 (2018).

[16] T. P. Le, J. Levinson, K. Modi, M. M. Parish, and F. A. Pollock, *Spin-chain model of a many-body quantum battery*, *Phys. Rev. A* **97**, 022106 (2018).

[17] D. Rossini, G. M. Andolina, D. Rosa, M. Carregá, and M. Polini, *Quantum advantage in the charging process of sachdev-ye-kitaev batteries*, *Phys. Rev. Lett.* **125**, 236402 (2020).

[18] R. Salvia, M. Perarnau-Llobet, G. Haack, N. Brunner, and S. Nimmrichter, *Quantum advantage in charging cavity and spin batteries by repeated interactions*, *Phys. Rev. Res.* **5**, 013155 (2023).

[19] Z. Beleño, M. F. Santos, and F. Barra, *Laser powered dissipative quantum batteries in atom-cavity qed*, *New J. Phys.* **26**, 073049 (2024).

[20] J.-s. Yan and J. Jing, *Charging by quantum measurement*, *Phys. Rev. Appl.* **19**, 064069 (2023).

[21] S.-f. Qi and J. Jing, *Magnon-mediated quantum battery under systematic errors*, *Phys. Rev. A* **104**, 032606 (2021).

[22] Y. Huangfu and J. Jing, *High-capacity and high-power collective charging with spin chargers*, *Phys. Rev. E* **104**, 024129 (2021).

[23] F. Zhao, F.-Q. Dou, and Q. Zhao, *Quantum battery of interacting spins with environmental noise*, *Phys. Rev. A* **103**, 033715 (2021).

[24] M. B. Arjmandi, H. Mohammadi, and A. C. Santos, *Enhancing self-discharging process with disordered quantum batteries*, *Phys. Rev. E* **105**, 054115 (2022).

[25] F. Barra, K. V. Hovhannisyan, and A. Imparato, *Quantum batteries at the verge of a phase transition*, *New J. Phys.* **24**, 015003 (2022).

[26] L. Gao, C. Cheng, W.-B. He, R. Mondaini, X.-W. Guan, and H.-Q. Lin, *Scaling of energy and power in a large quantum battery-charger model*, *Phys. Rev. Res.* **4**, 043150 (2022).

[27] S. Ghosh and A. Sen(De), *Dimensional enhancements in a quantum battery with imperfections*, *Phys. Rev. A* **105**, 022628 (2022).

[28] Y. Yao and X. Q. Shao, *Optimal charging of open spin-chain quantum batteries via homodyne-based feedback control*, *Phys. Rev. E* **106**, 014138 (2022).

[29] Y.-Y. Zhang, T.-R. Yang, L. Fu, and X. Wang, *Powerful harmonic charging in a quantum battery*, *Phys. Rev. E* **99**, 052106 (2019).

[30] A. Crescente, M. Carregá, M. Sassetto, and D. Ferraro, *Ultrafast charging in a two-photon dicke quantum battery*, *Phys. Rev. B* **102**, 245407 (2020).

[31] A. Crescente, M. Carregá, M. Sassetto, and D. Ferraro, *Charging and energy fluctuations of a driven quantum battery*, *New J. Phys.* **22**, 063057 (2020).

[32] N. Friis and M. Huber, *Precision and work fluctuations in gaussian battery charging*, *Quantum* **2**, 61 (2018).

[33] G. M. Andolina, D. Farina, A. Mari, V. Pellegrini, V. Giovannetti, and M. Polini, *Charger-mediated energy transfer in exactly solvable models for quantum batteries*, *Phys. Rev. B* **98**, 205423 (2018).

[34] W.-X. Guo, F.-M. Yang, and F.-Q. Dou, *Analytically solvable many-body rosen-zener quantum battery*, *Phys. Rev. A* **109**, 032201 (2024).

[35] S. Gherardini, F. Campaioli, F. Caruso, and F. C. Binder, *Stabilizing open quantum batteries by sequential measurements*, *Phys. Rev. Res.* **2**, 013095 (2020).

[36] A. C. Santos, B. i. e. i. f. m. c. Çakmak, S. Campbell, and N. T. Zinner, *Stable adiabatic quantum batteries*, *Phys. Rev. E* **100**, 032107 (2019).

[37] A. Rojo-Francàs, F. Isaule, A. C. Santos, B. Juliá-Díaz, and N. T. Zinner, *Stable collective charging of ultracold-atom quantum batteries*, *Phys. Rev. A* **110**, 032205 (2024).

[38] D. Rosa, D. Rossini, G. M. Andolina, M. Polini, and M. Carregá, *Ultra-stable charging of fast-scrambling syk quantum batteries*, *J. High Energy Phys.* **2020**, 67 (2020).

[39] D. Farina, G. M. Andolina, A. Mari, M. Polini, and V. Giovannetti, *Charger-mediated energy transfer for quantum batteries: An open-system approach*, *Phys. Rev. B* **99**, 035421 (2019).

[40] B. Ahmadi, P. Mazurek, P. Horodecki, and S. Barzanjeh, *Nonreciprocal quantum batteries*, *Phys. Rev. Lett.* **132**, 210402 (2024).

[41] P. Chen, T. S. Yin, Z. Q. Jiang, and G. R. Jin, *Quantum enhancement of a single quantum battery by repeated interactions with large spins*, *Phys. Rev. E* **106**, 054119 (2022).

[42] M. T. Mitchison, J. Goold, and J. Prior, *Charging a quantum battery with linear feedback control*, *Quantum* **5**, 500 (2021).

[43] P. Sathe and F. Caravelli, *Universally-charging protocols for quantum batteries: A no-go theorem*, (2024), arXiv:2409.02198 [quant-ph].

[44] H. J. Carmichael, *Dissipation in quantum mechanics: The master equation approach*, in *Statistical Methods in Quantum Optics 1: Master Equations and Fokker-Planck Equations* (Springer Berlin Heidelberg, Berlin, Heidelberg, 1999) pp. 1–28.

[45] A. F. Kockum, A. Miranowicz, V. Macrì, S. Savasta, and F. Nori, *Deterministic quantum nonlinear optics with single atoms and virtual photons*, *Phys. Rev. A* **95**, 063849 (2017).

[46] J. Joo, J. Bourassa, A. Blais, and B. C. Sanders, *Electromagnetically induced transparency with amplification in superconducting circuits*, *Phys. Rev. Lett.* **105**, 073601 (2010).

[47] V. E. Manucharyan, J. Koch, L. I. Glazman, and M. H. Devoret, *Fluxonium: Single cooper-pair circuit free of charge offsets*, *Science* **326**, 113 (2009).

[48] A. E. Allahverdyan, R. Balian, and T. M. Nieuwenhuizen, *Maximal work extraction from finite quantum systems*, *Europhys. Lett.* **67**, 565 (2004).

[49] D. F. James and J. Jerke, *Effective hamiltonian theory and its applications in quantum information*, *Can. J. of Phys.* **85**, 625 (2007).

[50] O. Gamel and D. F. V. James, *Time-averaged quantum dynamics and the validity of the effective hamiltonian model*, *Phys. Rev. A* **82**, 052106 (2010).

[51] W. Shao, C. Wu, and X.-L. Feng, *Generalized james' effective hamiltonian method*, *Phys. Rev. A* **95**, 032124 (2017).

[52] F. Reiter and A. S. Sørensen, *Effective operator formalism for open quantum systems*, *Phys. Rev. A* **85**, 032111 (2012).

[53] F. Campaioli, J. H. Cole, and H. Hapuarachchi, *Quantum master equations: tips and tricks for quantum optics, quantum computing, and beyond*, *PRX Quantum* **5**, 020202 (2024).